Comparison of density of stainless steel 316L parts produced with selective laser melting using different powder grades

A. B. Spierings*, G. Levy*
*institute for rapid product development irpd, inspire AG, Lerchenfeldstrasse 5, CH-9014 St.Gallen

Reviewed, accepted 9/15/09

Abstract:
Selective Laser Melting is a powder based additive manufacturing process where the metallic powder particles are fused to 3D parts using a high energy laser beam. Much work has already been conducted to investigate the details of the process, suitable materials and process parameters and further more. As metallic powders are the raw material for this process, there are still a lot of open questions relating to suitable grain size distributions for dense parts with regard to productivity, surface quality, mechanical strength and ductility. The present work shows the results of density measurements of parts, produced using three different particle size distributions and different energy densities of the laser beam. Two layer thicknesses of 30µm and 45µm were investigated.
It is shown that without a minimal amount of fine grains, which are able to fill the voids between the coarse grains, lower scan speeds are needed in order to produce dense parts. Furthermore, the differences in the relation of the powders to the densities, the layer thicknesses and laser scan speeds indicate, that the powder grain size distribution plays an important role and that should be taken into account for optimal results. This work is a contribution to the ASTM initiative F42 for "Additive Manufacturing".

I. Introduction

Looking back to the development directions of conventional production technologies like drilling and milling, rapid technologies designate a logical development stage towards further integration of computer technologies into the production processes [1]. In the very beginning of industrial production, extensive manual labour was predominant for hundreds of years. The invention and integration of electric motors into the production processes led to a huge increase of productivity, accuracy and repeatability. The next important step was the invention of electric control systems, which further improved the reliability of the processes. Nevertheless, manual work was and is still important, although many preparation tasks for production can be done at the desktop and the production processes are usually fully computer controlled.
The next step towards a further integration of computer techniques into the production processes was laid by the additive manufacturing processes. These technologies need only a CAD data set of the item to build. Therefore, no further programming steps e.g. of the production machines have to be undertaken – it is a fully integrated process from data generation (CAD) over process planning, parameterisation to the self running production [2]. As a consequence, by reducing manual efforts to a minimum, these techniques have the potential for the next step towards higher productivity.
The group of corresponding additive production processes [3] include Selective Laser Sintering and Selective Laser- or Electron Beam Melting; so powder bed based processes to create plastic or metallic parts, respectively. Other similar processes are for example stereo lithography and 3D printing, which uses a fluid resin or a photopolymer, respectively, to build up parts.
Today, additive manufacturing processes like e.g. SLS and 3D Printing, tend towards Rapid Manufacturing (RM), where the parts produced are used directly in the end application and not only as a prototype. The SLM process would be perfectly usable for RM, as the metallic parts produced provide high material strength [3, 4] due to the achievable density of nearly 100% by

fully melting the particles [4]. Furthermore, the industry requires metallic materials for RM [5]. Although SLM parts can be used in a wide field of applications like medical implants [6-10], mechanical engineering [11] and aerospace industry [12], there are still many challenges to be solved for a real rapid manufacturing. Beside others, these challenges include the part orientation, layering strategy, support generation and structure, process speed and control facilities [5], which have to be considered in the future [13]. By improving these subjects, additive processes for producing metallic parts (SLM, EBM) could be some when considered as real RM-processes in the future.
Over all, today additive processes can be considered as entering the standardisation stage [3, 14] as first RM applications have already been conducted successfully [15, 16]. This is underlined by first efforts for an international standardisation by ISO [17, 18] and ASTM. The later has started the initiative F42 for Additive Manufacturing Processes in 2008.
This paper is a contribution to open questions in the field of Selective Laser Melting. Even for stainless steel 316L, there are a number of different sources available providing powers with different particles size distributions. Furthermore, the layer thicknesses of the parts to be produced vary between 30µm and about 60µm, depending on the application, the geometry, the machine used and the preferences of the operator. The paper presents results concerning differences in achievable densities using three different particles size distributions using layer thicknesses of 30µm and 45µm. The results contribute also important information to current standardisation initiatives (ASTM).

II. Methods, Materials and Measurements

a) SLM Machine

Metallic parts have been produced using a SLM machine of Concept Laser GmbH, Germany, type M1 (2005). This machine is equipped with a Q-switched Nd: YAG diode-pumped solid state laser source of Rofin-Sinar Laser GmbH. This laser provides a continuous laser beam with a wavelength of 1064 nm, the spot size is 0.2mm and the nominal laser power at the building platform is in the range up to about 104W ± 0.5W.
The machine software uses a specific scan strategy where the cross sections of the geometries are divided into 5mm x 5mm squares. Each square is shifted from layer to layer by 1 mm in x- and y-direction. Furthermore, the squares are rotated by 45° to the x- or the y-direction of the building platform. These arrangements allow it to minimise any isotropy in x- and y-direction.

b) Materials

Each test cube was produced in 316L stainless steel, whereas three different particles size distributions were used (Table 1). The grain size distributions were measured using a HELOS&RODOS R3 Laser Diffraction Sensor of Sympatec GmbH.

Powder No.	316L – Type 1	316L – Type 2	316L – Type 3
D_{10} [µm]	6.3	19.91	15.64
D_{50} [µm]	15.05	28.19	37.00
D_{90} [µm]	30.79	41.31	59.69
D_{50} / D_{10}	2.4	1.4	2.4
Tap density [$^{g}/_{cm}3$]	4.8	4.6	4.7
Relative powder density	≈ 60.1%	≈ 57.6%	≈ 58.9%
Span S [-] [19]	1.63	0.76	1.19

Table 1: 316L powders used for producing the test cubes.

The powders are characterised in the following way: Powder type 1 and 2 (Figure 3) can be characterised by a typical Gaussian like grain size distribution with a slight asymmetry towards coarser grains where as type 3 (Figure 3) is an asymmetric distribution with an increased concentration of finer grains. Furthermore, the particles are not as spherical as e.g. type 1 and in comparison the maximal grain sizes are much bigger. Although type 1 has a significant higher amount of fine particles, the flowability of the powder, which has not been measured, is still acceptable.

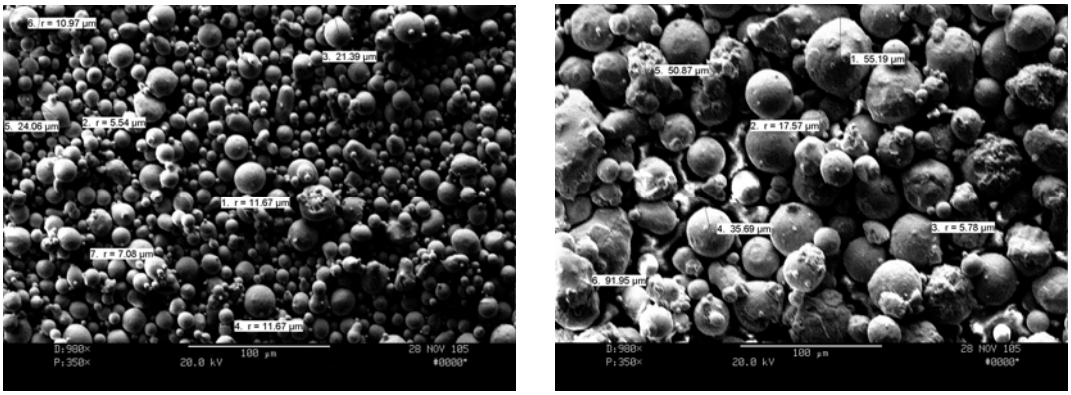

Figure 1: SEM picture of powder type 1 (left) and type 3 (right)

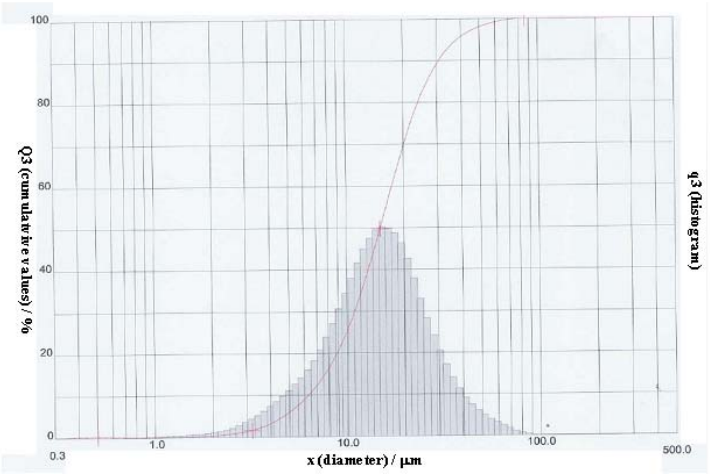

Figure 2a: Size frequency and cumulative size frequency of powder type 1

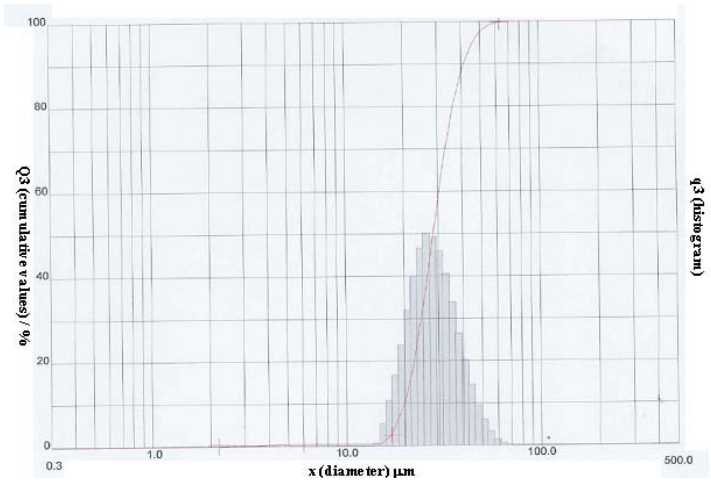

Figure 2b: Size frequency and cumulative size frequency of powder type2

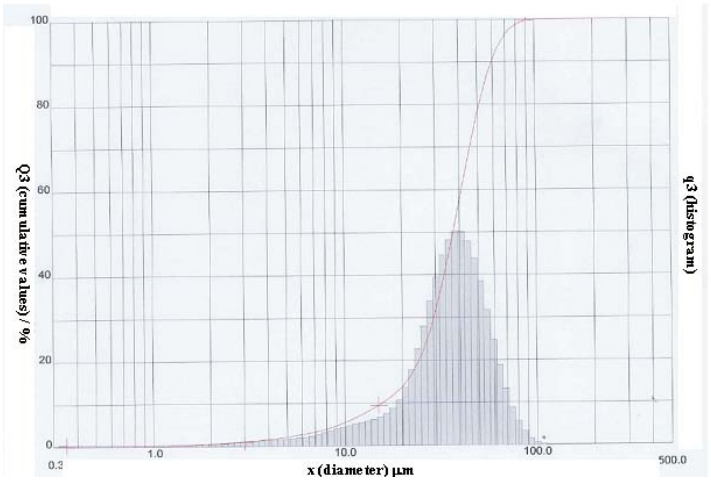

Figure 2c: Size frequency and cumulative size frequency of powder type 3

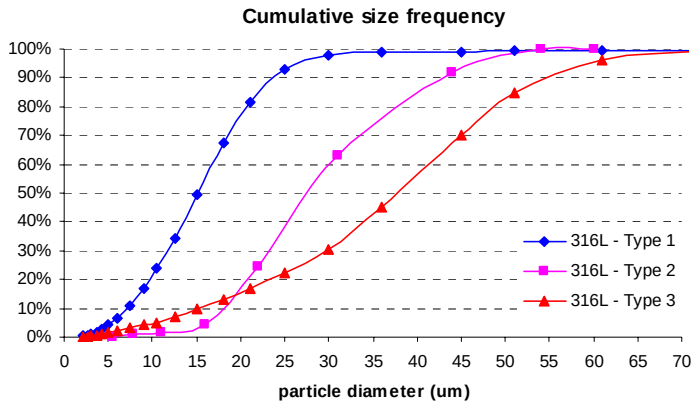

Figure 3: Cumulative size frequencies of powder type 1, 2 and 3

c) Process parameters for test cubes

In order to produce parts with the highest possible density in combination with a low surface roughness, it is important to optimise for a specific material the most important influencing parameters. These parameters can be divided into four groups: Material specific parameters (grain size distribution, flow properties etc), laser parameters (laser power, spot size etc.), scan parameters (scan velocity, hatching distance, etc.) and environmental parameters (ambient temperature, protective gas atmosphere, O_2 level). These four groups of parameters are listed in more detail in [20].
The current machine setup allows only the adaption of scan speed, laser power, hatching distance (Table 2), and some more, less important parameters. The cubes produced have a dimension of $12x12x12mm^3$ and were produced with the processing parameters according to Table 2. The ambient temperature was approximately 40°C as there is no preheating of the powder or the process chamber. The O_2-level during the SLM process was between 0.3% and 0.8%.

Materials	316L – Type 1	316L – Type 2	316L – Type 3
Layer thickness t_{Layer} [µm]	30	30	30
Laser Power[1] P_{Laser} [W]	104	104	104
Scanning speed[2] v_{Scan} [$^{mm}/_{s}$]	300 – 800[2]	250 - 500	250 - 500
Hatch distance s_{Hatch} [mm]	0.13	0.13	0.13

Table 2: Processing parameters for the production of test cubes
[1] Laser power approximately 104W ± 0.5W
[2] The scan speed was adjusted in steps of 25 $^{mm}/_{s}$ or 50 $^{mm}/_{s}$

A layer thicknesses t_{Layer} of 30µm was used as this thickness typically leads to good the surface qualities of the parts produced and stair effects are minimal [20]. The laser power P_{Laser} was set to the maximum possible power in order to maximise the scan velocity and productivity, respectively. Expecting better density values for powder Type 1 compared to the coarser powders, the scan speed range was set somewhat higher than for powder types 2 and 3. A driving parameter for the density of SLM-parts is the energy density E_d [20], which includes all above mentioned process parameters:

$$E_d = \frac{P_{Laser}}{v_{scan} \cdot s_{Hatch} \cdot t_{Layer}} \qquad (1)$$

With P_{Laser} the laser power, v_{scan} the scan velocity, s_{Hatch} the hatching distance and t_{Layer} the layer thickness.
T_{Spot} [19] describes the time dependency of the melting process and related effects like e.g. the temperature dependence of the melt viscosity, with d_s the spot size diameter:

$$T_{spot} = \frac{d_S}{v_{Scan}} \qquad (2)$$

d) Density measurement for bulk test cubes

The density of a SLM-part was measured using the Archimedes method [21], which allows to measure the mean density of any complex geometry, as not only single cross-sections are taken into account but the whole volume of a part. For conducting the measurements, a Mettler balance (Type AE200) with a specific density measurement device for solid materials (Type AB33360) was used. The calculation of the density ρ_p of the part under consideration follows equation (1):

$$\rho_p = \frac{m_a}{m_a - m_{fl}} \cdot \rho_{fl} \qquad (3)$$

ρ_{fl} is the density of the fluid, which is temperature dependent, ma is the mass of the part in air and m_{fl} is the mass of the part in the fluid. The measurements were conducted with de-ionised water. The temperature-dependence of the fluid [22] was taken into account.

III. Results and Discussion

a) Considerations to powder layer density

For Additive Manufacturing Powder Processes such as SLS and SLM, the powder layer density should be as high as possible [19] in order to produce dense parts with high scan velocities and therefore with high productivity. The density of a powder layer is mainly dependent on the particle sizes or size distributions, respectively. If the amount of fine particles, e.g. in the range of about 5µm or less, is too high, the agglomeration of particles can eliminate their positive effects of filling up voids. McGeary [23] showed in his experiments that a bi-modal mixture of powders with a size ration of 1:7 can increase the powder density by about 30%, if the amount of fine particles reaches 30%.

Regarding the density of thin powder layers, as used for SLS and SLM, the situation is different compared to typical density measurements of powders (apparent and tap density) [19]. The reason is that the particle diameters typically can be in the same range as the powder layer thicknesses (e.g. 30µm and 45µm as in this study). Karapatis [19] showed that the additional amount of voids, caused by the platform, can cause as much as 40% of the total porosity of the powder bed. This amount tends to 0 the thicker the layer is. Therefore, it is generally helpful to use particle size distributions where the fine particles can fill the voids between the bigger particles. Furthermore, spherical particles are preferred for high packing density since they exhibit low interparticle friction and high mobility [24].

The measurement of the real density of a thin powder layer is very difficult. Karapatis [19] described in his experiments that the layer can be compacted by the deposition system used and that the layer density can be increased to values higher than apparent or tap densities. An optimum ratio of 10 particles per layer thickness leads to a layer density of more than 60%, which is slightly more than the measured tap density of the powders used in this study.

Real powder layer thickness t_{eff}

Assuming a powder layer density of 60% (Table 1) within the first generated 30µm layer, the scanning to a material density of e.g. 99% leads by shrinkage in the vertical direction to a scanned layer thickness of 18.2µm. Together with lowering the building platform by 30µm, the resulting next powder layer thickness is 41.8µm. After building less than 10 layers (Figure 4), the real, by the deposition system generated powder layer thickness reaches a stable value of 49.5µm (for 60% powder layer density), which is then scanned to a bulk layer thickness of 30µm. This effective layer thickness t_{eff} is overlapped by the surface roughness, which is typically between about 7µm and about 15µm [10, 25] for R_a or between 25µm and about 40µm R_z, respectively.

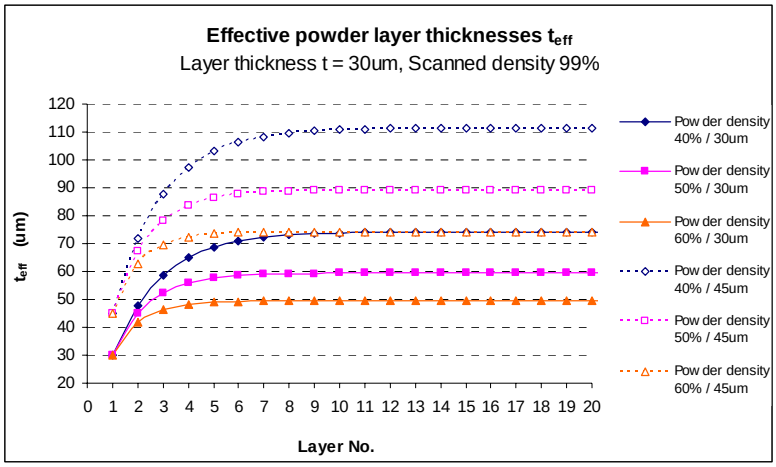

Figure 4: Development of the effective powder layer thickness t_{eff} for scanned layer thicknesses of 30µm and 45µm and powder layer densities of 40%, 50% and 60%.

These increased powder layer thicknesses affect the optical and thermal properties of the whole layer and therefore the consolidation process. The optical penetration depth, which describes the depth at which the laser intensity equals the incident intensity be e, is about 63µm, measured for a fine titanium powder [26], indicating that this distance is just in the range or somewhat bigger than the effective layer thickness.
Furthermore, within the first about 6 to 10 layers the real thickness of the structure being built is smaller than the theoretical thickness of these first layers. Using the situation above, the difference within the first 7 layers is about 20µm. As this difference is typically within a part-specific support structure, the part itself is not affected by these inhomogeneous layer thicknesses so that its dimensional accuracy in the vertical z-direction is given.

b) Part Density
In order to get insight into the fluctuation range of density measurements, three samples produced with the same process parameters were measured four times each. The mean density of these parts was 99.53% and the standard deviation of the density measurements was 0.082%. A repetition was performed using slightly changed process parameters, which resulted in a mean density of 99.33% and a standard deviation of 0.070%.
If the amount of energy, which is brought into this powder layer is sufficient high to fully melt all the powder particles, nearly fully dense parts are producible with all three powder types. Due to the different powder characteristics (Table 1), the scan velocities for dense parts can vary significantly.

Layer thickness 30µm
With 30µm layers it is possible to produce parts with very high densities (> 99%, typically about 99.5%) if enough energy is available to fully melt the powder particles. The lower the energy densities) are the lower are the part densities, as reported by [21].
A further parameter affecting the solidification behaviour is the time constant (equ. 2) of the process, which has to be high enough compared to typical time dependent physical effects of a melt pool like e.g. the break up time of a scan track. As soon as $t_{Spot} >\approx 0.0035$s nearly fully dense parts are possible (Figure 6) with all powder types. This is nearly one order of magnitude longer than the typical break up time of a melt pool [27].

As expected, Figure 5 shows that the density is also highly dependent on the powder characteristics. Regarding the 30µm layers, it is obvious that the coarser powders typically result in lower density values at a specific energy density. There are two main factors influencing porosity: First, the energy supplied might not be sufficient to fully melt the bigger particles. Therefore, these particles can remain, especially at the lower not irradiated sides, partially unmelted, which generates voids within the scanned layer. A second, indirect effect is the emerging surface roughness of parts, produced with coarse powders. Coarse powder particles are not able to fill the valleys between the scan tracks of the last layer, which generates also voids. So, if the amount of fine particles is big enough, mentioned voids can be partially filled and easily be melted by heat conduction.
Although the biggest particles of powder type 3 are bigger than the ones of type 2, the fact of the existence of an amount of fine particles in powder type 3 explains the better part density behaviour: The amount of particles with a diameter smaller than about 10µm to 15µm is significantly higher for powder type 3 than for powder type 2 (Figure 2), although D_{10} is in the same range for type 2 and type 3.

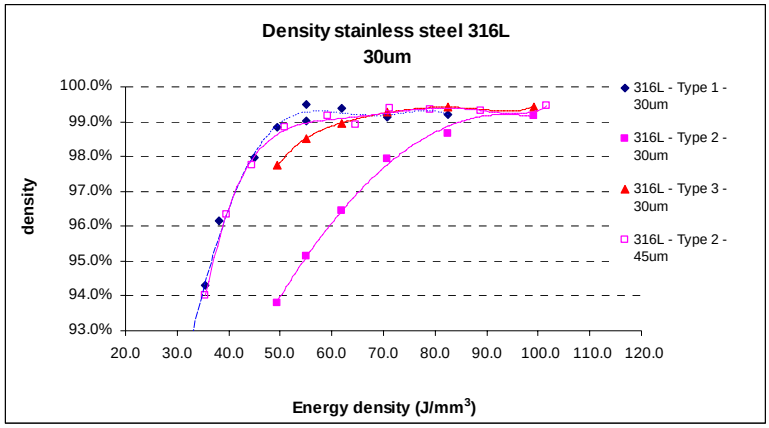

Figure 5: Dependence of the part density of powder type and energy density for 30µm layers and for 45µm layer of powder type 2

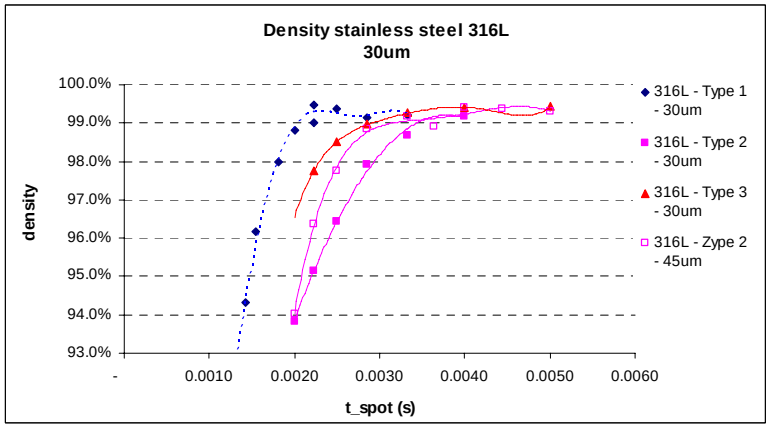

Figure 6: Part density in dependence of the spot time

Layer thickness 45µm

In contrast to the 30µm layers, the densities of the 45µm layers are - for a specific energy density or scan speed, respectively - in the range of about 1% lower for all three powder types (Figure 7). This can be expected and is obvious as the energy flux is reduced quickly the thicker the powder layers are [28]. Interestingly and in contrast to the 30µm layers, powder type 2 shows for all scan speeds a better density than powder type 3. This could be explained by the fact that the effective layer thickness for 45µm layers reaches up to about 74µm (Figure 4). As all particles are smaller than this effective thickness, the amount of fine powder grains becomes comparatively less important. It is more important to consider the amount of bigger particles and their diameters. Regarding this, powder type 3 has the biggest particles, which need more energy to get fully molten. Therefore, the corresponding part densities are lower than for powders with finer grains. Figure 5 shows that the densities of the 45µm / powder type 2 measurements are almost identical to the 30µm / powder type 1 values. The better values of a 45µm-layer processed with powder type 1 (Figure 7) is explained by the fact that the comparatively lower scan speeds allow more time for heat conduction and therefore a better melting process of the fine particles.

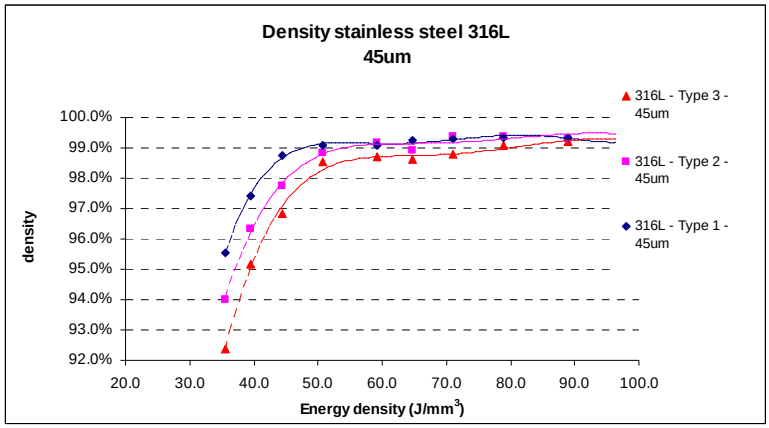

Figure 7: Dependence of the part density of powder type and energy density for 45µm layers

c) Discussion

The results of this study indicate that it is possible to produce parts with a high density (≈ 99.5%) using all three different grain size distributions, when the scan speeds are adjusted adequately. If the particle size distribution does not fulfil some basic requirements [24], the adjustments of the process parameters typically affect the productivity of the SLM process in a negative way.

One has to be aware that a remaining porosity in the range of about 0.5% can not be avoided in powder bed based processes like Selective Laser Melting or Selective Laser Sintering. There will always be a remaining porosity in the parts produced. The goal is to minimise this remaining porosity, where as the definition of an acceptable porosity is dependent on the process of comparison.

Looking at the SLM process and current results, the achievable densities are at least as good or better than the densities of parts produced with other forming production techniques like e.g. Metal Injection Moulding [29, 30] or casting.

The porosity of additive manufactured parts is affected by several influencing parameters:

- Material type:
  Different materials, such as steel, Ti, CoCr, and Aluminum highly affect, due to their specific physical behaviour, the details of the melting process and therefore of the binding mechanism [31]. However, the general results and dependencies are valid for all types of metal materials [10, 20, 32].

- Powder type:
  - Grain size distribution: Relevant powder parameters are at least D_{10}, D_{50} and D_{90}.
  - The powder bed density [19, 24], which is affected by the grain size distribution and the coating system (ruler, flexible coating system, roller), should be as high as possible.
  - The effective powder layer thickness (Figure 4).

Karapatis [24] derived criteria for suitable particle size distributions, using readily available numbers:

$$D_{90} < t_{Layer} \quad , \quad \frac{D_{50}}{D_{10}} \geq 10 \quad , \quad \frac{D_{90}}{D_{10}} \leq 19 \qquad (4)$$

These equations indicate that 50% of the particles are 10 times coarser than the 10% finer grains and that about 20% of the particles sizes are in a 1:20 ratio. The requirements have been found basically on investigations for bi-modal powder size distributions and adapted for mono-modal powders.
However, for the powders used in this study, the second requirement is not fulfilled as this ratio is between 1.4 and 2.4 (Table 1) and the third requirement is not fulfilled either. Furthermore, although there are significant differences between powder Type 1 and Type 3, the D_{50}/D_{10} – ratio is about the same.

IV Conclusion

Additional requirements for thin powder layers have to be defined in order to assess adequately typically available powders for SLM. It is difficult to generate general requirements based on the three available different powder size distributions used in this study. Any requirement should be able to assess the quality of powders considering flowability and resulting part density and productivity (scan speed) in a SLM process. Nevertheless, some basic requirements for powders are presented. It is assumed that

- $\frac{t_{eff}}{D_{90}} \approx 1.5$
  This indicates that the effective powder layer thickness t_{eff} is at least 50% higher than the diameter of 90% of the powder particles. Therefore, most of the particles can be deposited within t_{eff}.

- $\frac{D_{90}}{D_{10}} \approx 5$
  This requirement asks for a sufficient amount of fine particles, which are able to fill the voids between the coarser grains. Both requirements together indicate that D_{10} is about 7.5 times smaller than t_{eff}.

In addition to these requirements, which address the part density and the productivity of the process, upper limitations exist for the amount of fine particles. If D_{10} is below about 5µm to 6 µm, agglomeration of the powder particles starts to occur. This reduces the flowability of the powder so that it becomes more and more difficult to create appropriate, homogeneous powder layers with a high powder layer density [19]. Therefore, Karapatis requires that the Haussner ratio is below 1.25 [19, 33]. However, ρ_{tap} and $\rho_{apparent}$ are not always available. Further work has to be done in order to define suitable and easily measurable values for different powders.

Outlook

Besides part density and productivity, the resulting mechanical strength and ductility is also affected by the powder type. Furthermore, it can be assumed that a coarser powder leads to a rougher surface quality, especially when some coarse powder grains are not fully melted by the laser beam. Therefore the investigations into the influence of different powders on mechanical parameters and surface quality are driven further in order to define suitable powders for SLM.

Acknowledgement

The authors want to thank Mr. A. Frauchiger for his help in conducting needed trials on the SLM machine and part density measurements.

Literature

1. Spierings, A.B. and G. Levy. *Rapid Manufacturing - auch mit SLM*. in *Rapid.Tech*. 2009. Erfurt, Germany: Messe Erfurt AG.
2. Müller, D.H. and H. Müller, *Rapid Prototyping Verfahren - Eigenschaften, Anwendung und Verbreitung*. 2002, Bremer Institut für Betriebstechnik und angewandte Arbeitswissenschaft an der Universität Bremen - BIBA: Bremen.
3. Levy, G.N., R. Schindel, and J.P. Kruth, *RAPID MANUFACTURING AND RAPID TOOLING WITH LAYER MANUFACTURING (LM) TECHNOLOGIES, STATE OF THE ART AND FUTURE PERSPECTIVES.* CIRP Annals - Manufacturing Technology, 2003. **52**(2): p. 589-609.
4. Kruth, J.P., et al., *Binding mechanisms in selective laser sintering and selective laser melting.* Rapid Prototyping Journal, 2005. **11**(1): p. 1355-2546.
5. Munguía, J. *Persuing successful Rapid Manufacturing in a standards-less industry: a best practice approach*. in *Advanced Research in Virtual and Rapid Prototyping*. 2007. Leiria, Portugal: Taylor&Francis.
6. Abe, F., et al., *Influence of forming conditions on the titanium model in rapid prototyping with the selective laser melting process.* Proceedings Of The Institution Of Mechanical Engineers Part C-Journal Of Mechanical Engineering Science, 2003. **217**(1): p. 119-126.
7. Dalgarno, K.W., et al., *Mass Customisation of Medical Devices and Implants: State of the Art and Future Directions.* 2006.
8. Murr, L.E., et al., *Microstructure and mechanical behavior of Ti-6Al-4V produced by rapid-layer manufacturing, for biomedical applications.* Journal of the Mechanical Behavior of Biomedical Materials, 2009. **2**(1): p. 20-32.
9. Tolochko, N.K., et al., *Dental root implants produced by the combined selective laser sintering/melting of titanium powders.* Proceedings Of The Institution Of Mechanical Engineers Part L-Journal Of Materials-Design And Applications, 2002. **216**(L4): p. 267-270.
10. Vandenbroucke, B. and J.P. Kruth, *Selective Laser Melting of biocompatible metals for rapid manufacturing of medical parts.* Rapid Prototyping Journal, 2007. **13**(14): p. 196-203.
11. Spierings, A.B. and G. Levy, *Rapid Manufacturing (RM) und Selective Laser Melting (SLM) - Eine zukunftsträchtige Fertigungstechnologie*. 2008, NC-Gesellschaft N.V. - Anwendung Neuer

Technologien: Wangen.
12. Rochus, P., et al., *New applications of rapid prototyping and rapid manufacturing (RP/RM) technologies for space instrumentation.* Acta Astronautica, 2007. **61**(1-6): p. 352-359.
13. Bourell, D.L., M.C. Leu, and D.W. Rosen, *Roadmap for Additive Manufacturing - Identifying the Future of Freeform Processing*, ed. D.L. Bourell. 2009, Austin: The University of Texas at Austin - Laboratory for Freeform Fabrication.
14. Wohlers, T., *Is Rapid Manufacturing Real?*, in *Time-Compression Technologies*. 2005.
15. Klare, M. and R. Altmann, *Rapid Manufacturing in der Hörgeräteindustrie.* RTejournal, 2005. **2**: p. 104-120.
16. Schweiger, J., *Rapid Prototyping - Neue Fertigungswege in Zahntechnik und Zahnmedizin*, in *digital_dentalnews*. 2008. p. 36-41.
17. ISO/DIS, *Plastics - Preparation of test specimens of thermoplastic materials using mouldless technologies -- Part 1: General principles, and laser sintering of specimens*. 2008.
18. VDI, V.D.I., *Generative Fertigungsverfahren - Rapid Technologien (Rapid Prototyping)*, in *Grundlagen, Begriffe, Qualitätskenngrössen, Liefervereinbarungen*. 2007.
19. Karapatis, N.P., *A sub-process approach of selective laser sintering*. 2002, Ecole Polytechnique fédérale de Lausanne EPFL: Lausanne.
20. Kruth, P.d.i.J.P., B. Vandenbroucke, I.J. Vaerenbergh van, and I. Naert, *Rapid Manufacturing of Dental Prostheses by means of Selective Laser Sintering/Melting*, in *Proceedings of the AFPR, S4*. 2005.
21. Over, C., *Generative Fertigugn von Bauteilen aus Werkzeugstahl X38CrMoV5-1 und Titan TiAl6V4 mit "Selective Laser Melting"*. 2003, RWTH Aachen: Aachen.
22. Sartorius, *Handbuch wägetechnische Applikationen: Teil 1 - Dichte*. 1999.
23. McGEARY, R.K., *Mechanical Packing of Spherical Particles.* Journal of the American Ceramic Society, 1961. **44**(10): p. 513-522.
24. Karapatis, N.P., G. Egger, P.-E. Gygax, and G. Glardon. *Optimization of Powder Layer Density in Selective Laser Sintering*. in *Proc. Of the 9th Solid Freeform Fabrication Symposium*. 1999. Austin (USA).
25. Rossi, S., F. Deflorian, and F. Venturini, *Improvement of surface finishing and corrosion resistance of prototypes produced by direct metal laser sintering.* Journal Of Materials Processing Technology, 2004. **148**(3): p. 301-309.
26. Fischer, P., et al., *A model for the interaction of near-infrared laser pulses with metal powders in selective laser sintering.* Applied Physics A: Materials Science & Processing, 2002. **74**(4): p. 467-474.
27. Rombouts, M., J.P. Kruth, L. Froyen, and P. Mercelis, *Fundamentals of Selective Laser Melting of alloyed steel powders.* CIRP Annals - Manufacturing Technology, 2006. **55**(1): p. 187-192.
28. Gusarov, A.V. and J.P. Kruth, *Modelling of radiation transfer in metallic powders at laser treatment.* International Journal Of Heat And Mass Transfer, 2005. **48**(16): p. 3423-3434.
29. Heaney, D.F., T.J. Mueller, and D. P.A., *Mechanical properties of metal injection moulded 316l stainless steel using both prealloy and master alloy techniques.* Powder Metallurgy, 2004. **7**(4): p. 1-7.
30. Johnson, J.L. and D.F. Heaney, *Metal Injection Molding of Co-28Cr-6Mo*, Center for Innovative Sintered Products Penn State University. p. 1-5.
31. Kruth, J.P., G. Levy, F. Klocke, and T.H.C. Childs, *Consolidation phenomena in laser and powder-bed based layered manufacturing.* CIRP Annals - Manufacturing Technology, 2007. **56**(2): p. 730-759.
32. Santos, E.C., et al., *Microstructure and mechanical properties of pure titanium models fabricated by selective laser melting.* Proceedings Of The Institution Of Mechanical Engineers Part C-Journal Of Mechanical Engineering Science, 2004. **218**(7): p. 711-719.
33. Geldart, D., E.C. Abdullah, and A. Verlinden, *Characterisation of dry powders.* Powder Technology, 2009. **190**(1-2): p. 70-74.